Journal of the European Ceramic Society 21 (2001) 1061–1071

www.elsevier.com/locate/jeurceramsoc

Modelling of damage development during sintering

A. L. Maximenko, O. Van Der Biest *

Departement of Metallurgy and Materials Engineering, Katholieke Universiteit Leuven, W. De Croylaan 2, BE-3001 Heverlee, Belgium

Received 16 December 1999; received in revised form 27 October 2000; accepted 30 October 2000

Abstract

A model for prediction of damage development during sintering is put forward. The model is based on the homogenization of sintering behaviour of a single neck between particles over all necks in material. The damage is treated as broken necks. Numerical analysis is based on a finite element implementation of a macroscopic extremum statement of the problem. The model predicts the volume distribution and evolution of damage in powder compacts under constrained sintering. Despite the generally justified consolidating role of sintering some examples of the existence of stable damage zones in materials are considered. © 2001 Elsevier Science Ltd. All rights reserved.

Keywords: Composites; Defects; Fracture; Modelling; Sintering

1. Introduction

Sintering of metal and ceramic powders is the crucial technological step for imparting strength to powder compacts. In general, sintering can be defined as a high-temperature process of matter redistribution encouraged by the free energy excess associated with the large free surface of fine particles in the powder compact. Decrease of the internal free surface during sintering leads, as a rule, to densification and strengthening of the compact. Nevertheless, in the case of the sintering of initially heterogeneous powder parts, the average densification and volume shrinkage of the part does not mean that all elements of the powder body are densified in the similar way or, at least some of them, densified at all. Heterogeneities in a sintering compact induce stresses when shrinkage rate differential exists. The stresses may cause local dilation of the powder elements, crack-like flaws or planar arrays of pores.

There exist abundant experimental observations of damage development during sintering. Appearance of a crack-like damage was detected for the sintering of particle films on a rigid substrate,[1] sintering of multilayer films,[2,3] sintering with rigid inclusions.[4,5] At the structural level of powder particles the breakage of junctures between particles was directly observed during sintering of ceramic composites and this effect even was specially termed as the "desintering phenomenon".[6] The destruction of necks between particles was also detected for the sintering of ordered particle structures,[7] initial solid-state sintering rearrangement of monosized two-dimensional particle arrays,[8] crack development in the constrained sintering films.[9]

In general, there is a close connection between damage development during sintering and fracture of discrete necks between particles. Experiments proved that damage appears actively only at early stages of sintering when contacts between particles are not strong enough.[10] At this stage discrete junctures between particles are readily discernible and sintering peculiarities of the powder body as a whole can be deduced from a plain superposition of the sintering behaviour of the independent discrete junctures.[11] According to this idea in the present article the damage is treated as broken necks between particles, the criterion of neck destruction is considered and anisotropic macroscopic model of powder material with broken necks is put forward. Within the model the evolution of damage during early stages of sintering can be followed.

The main specific feature of the damage development during sintering stems from the fact that the very sintering as a technological process is aimed at a healing of damage in the initially "destroyed into pieces" powder body. Therefore, any damage development is always accompanied and counteracted by damage healing. The

* Corresponding author. Tel.: +32-16-321-264; fax: +32-16-321-992.
E-mail address: omer.vanderbiest@mtm.kuleuven.ac.be (O. Van Der Biest).

PII: S0955-2219(00)00309-5

main objective of the modelling is to single out the special cases when damage can not be healed completely in a natural way of a free sintering. As a rule, the stable damage zones during sintering are the result of inappropriate geometrical structure of the powder based composites.

2. Deformational properties of a single contact between particles

At early sintering stage the analysis of the sintering behaviour of a single juncture between particles is a cornerstone for the construction of macroscopic model. In this case the macroscopic shrinkage rate of any element of powder compact can be treated as a result of homogenization over shrinkage rates of discrete junctures between the constituent particles.

As a rule, during sintering the relationship between exerted external stress in the neck area and shrinkage rate $\frac{\dot{w}}{R}$ has the following linear form[12]

$$\bar{\sigma} = \bar{\eta}\frac{\dot{w}}{R} - \bar{\sigma}_0 \tag{1}$$

where the bar above the parameters means normalization with respect to surface tension

$$\bar{\sigma} = \frac{\sigma R}{\gamma};\ \bar{\eta} = \frac{\eta R}{\gamma}$$

R is the particle radius, w is half the distance between particles (see Fig. 1), σ_0 is the sintering stress, η is the viscosity of the contact, γ is the surface energy and the point above the w means derivative with respect to time.

The values of the parameters in (1) are different for different sintering mechanisms. For the sintering of equal-sized spherical crystalline particles by grain-boundary and surface diffusion, the parameters have the following form[12]

$$\bar{\eta} = \frac{\tau_g}{\beta}\left(\frac{x}{R}\right)^2$$
$$\bar{\sigma}_0 = \frac{\alpha}{\beta}\frac{R^2}{x^2} \tag{2}$$

where x is the neck radius between particles, α, β are the dimensionless material constants, τ_g is the specific time of powder shrinkage due to the grain-boundary diffusion

$$\tau_g = \frac{\kappa T R^4}{\delta_g D_g \Omega \gamma} \tag{3}$$

where Ω is the atomic volume, T is the temperature, κ is the Boltzmann constant, δ_g, D_g are the grain boundary thickness and diffusivity, respectively. In general, parameters α, β are functions of parameter ξ

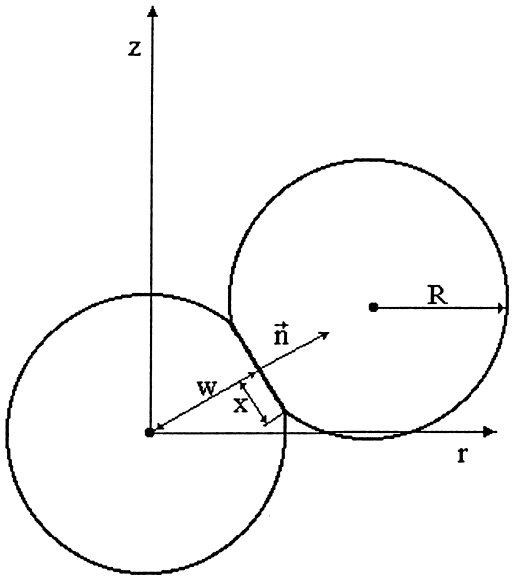

Fig. 1. Two-particle unit cell of sintered material.

$$\xi = \frac{\delta_g D_g}{\delta_s D_s} \tag{4}$$

where δ_s, D_s are the thickness of diffusion layer and diffusivity for the surface diffusion, respectively. According to[13] the contribution of lattice diffusion can be approximately incorporated into the model by the simple transformation of (4) into

$$\xi = \frac{\delta_g D_g + D_v R}{\delta_s D_s} \tag{5}$$

The rate of evolution of the neck radius between particles is also a linear function of the external stress. The equation for the neck radius rate has the form[12]

$$\frac{\dot{x}\tau_g}{R} = \frac{\phi}{(x/R)^5} - \frac{\vartheta\xi\bar{\sigma}}{(x/R)^3} \tag{6}$$

where ϑ, ϕ are the material parameters.

Let us assume that under some level of tensile loading the neck between particles can be broken. In the number of investigations devoted to the crack growth during constrained sintering[9] the condition of the neck area reduction was proposed to use as a fracture criterion. According to the criterion if neck area between particles decreases

$$\dot{x} < 0 \tag{7}$$

the instantaneous rupture of the neck is occurred. In reality, the diminution of the neck does not lead immediately to the neck destruction. Any neck between particles can

withstand some tensile strain even if (7) is valid. Moreover, direct modelling of the deformation of particle juncture predicts that neck reduction under tension is much slower process than initial neck growth to the same size.[14] It can be readily understood, because the neck reduction is governed only by the external tensile stress at the neck whereas the neck growth is substantially contributed also by the high initial curvature of the juncture between particles that accelerates diffusion. Therefore, the fracture criterion (7) is strictly correct only for the fracture of very small necks between particles, in all other cases it can just be treated as a necessary condition of damage development. In the ensuing presentation the criterion (7) will be used to specify sufficient conditions of the safe damage-free sintering.

If $\dot{\varepsilon}$ stands for the strain rate at the neck

$$\dot{\varepsilon} = \frac{\dot{w}}{R} \tag{8}$$

the criterion (7) can be rewritten in the form

$$\dot{\varepsilon} > \dot{\varepsilon}_c \tag{9}$$

where

$$\dot{\varepsilon}_c = \frac{\left(\frac{\phi\beta}{\vartheta\xi} - \alpha\right)}{\tau_g (x/R)^4} \tag{10}$$

Parameter $\dot{\varepsilon}_c$ can be treated as a positive tensile strain rate that should be applied to keep the neck area constant under sintering.

Despite its obvious limitations the criteria (7) or (9) often give a plausible assessments of damage development because in the most cases damage appears only at the very beginning of sintering process as a result of initial rearrangement of particles with very weak junctures. During the rest of the sintering the damage does not appears but it is only healed and criterion (7) is not necessary to use for large necks. Important advantage of the criterion (7) is its sensitivity to the sintering mechanisms. For example, the condition (9) cannot, practically, be met when surface diffusion mechanism dominates over grain boundary and lattice diffusion. It is usually the case at low sintering temperatures and, thus, criterion (9) explains why precoarsening of the powder at these temperatures turned out to be the effective way of damage elimination.[15]

If some evaluations of the maximum attainable tensile strain before neck fracture are known, the criterion (9) can be readily extended for that case. If neck is destroyed when the accumulated strain meets its critical value E_c it is sufficient to define critical strain rate as

$$\dot{\varepsilon}_c = \frac{E_c}{\Delta t} \tag{11}$$

instead of (10), where Δt is the time increment in numerical modelling of sintering evolution.

3. The model of powder material with broken necks between particles

At the step of transformation of the single contact stress-strain rate relationships into equations for the macroscopic behaviour of the powder body the dissipation energy approach of Ref. 11 was used. In this approach the derivation of the macroscopic stress-strain rate relationships is governed by the formation of the macroscopic dissipation function that is used as a potential function for the stresses with respect to strain rates.[16] The dissipation function is closely related to the density of the energy dissipation rate in a powder compact. The evaluation of the energy dissipation in the unit element of powder body was based on the assumption about affinity of the macroscopic and mesoscopic strain rate tensors. The term "mesoscopic" means the scale level of powder particles. Affinity implies that local strain rates of any particle array inside the macroscopic powder element are always identical to the average macroscopic strain rates of the powder element as a whole. According to the assumption, the velocities of the relative displacement for any pair of particles can be given as

$$\dot{X}_i = e_{ij} X_j \tag{12}$$

where X_i are the components of the center-to-center vector and e_{ij} are the components of the macroscopic strain rate tensor. Here and further the repeating indices mean summation. For spherical particles Eq. (12) can be rewritten to give the rate of the relative particle motion in the form

$$\dot{w} = \frac{1}{2} e_{ij} X_j n_i$$
$$X_j = 2 n_j w \tag{13}$$

where n_j are the components of the unit vector normal to the neck surface at the contact (see Fig. 1).

In order to obtain density of energy dissipation rate of the material as a function of e_{ij} one should summarize the dissipation rates over all junctures in the unit volume of material. Assuming that statistically all particles are the same one may calculate the dissipation rate per particle and multiply it on the number of particles in the unit volume. Therefore, the energy dissipation rate density of material I can be assessed through the dissipation rate per particle in the form[11]

$$I = \frac{\rho\gamma}{VR}\int_S \phi_c \bar{\sigma}\dot{w}dS \tag{14}$$

where ρ is the relative density of powder element, $\mathbf{V}, \mathbf{S}$ are the volume and surface of particle, respectively, $\frac{\rho}{V}$ is the number of particles in unit volume, ϕ_c is the fraction of particle surface in a contact with neighbour particles

$$\phi_c = 3\rho_0\frac{x^2}{R^2} + 9(1-\rho_0)\frac{x^4}{R^4} \tag{15}$$

where ρ_0 is the density of random close powder packing, that was taken equal to 0.64 in the calculations. Eq. (15) is a result of elimination of density from the formulas for $\frac{x}{R}$ and ϕ_c as density functions given in.[11] Contribution of friction forces between particles is not taken into account in (14). After substitution of (1) and (13) into (14) the energy dissipation rate (14) transforms into a function of macroscopic strain rates:

$$I = \frac{\rho\gamma}{VR}\int_{S_i} \phi_c\left[\frac{\bar{\eta}w^2}{R}e_{ij}e_{kl}n_in_jn_kn_l + we_{kl}\bar{\sigma}_0 n_k n_l\right]dS \tag{16}$$

Broken junctures between particles does not withstand tensile loading in the direction normal to the juncture's area. If some necks between particles are broken the tensile stress $\bar{\sigma}$ should be taken equal to zero for these necks. Affinity between macroscopic and mesoscopic deformational behaviour of the powder element assumes that fracture of just one juncture between particles is always accompanied by the fracture of all similarly oriented junctures within the element. It can be imagined as an instantaneous spreading of the crack parallel to the plane of the broken necks throughout the powder element.

Parameter S_i in (16) stands for the part of the particle surface with intact necks. The ratio

$$\chi = \frac{S - S_i}{S} \tag{17}$$

is proportional to the share of broken necks per particle and in subsequent development it is used as a damage parameter.

The evaluation of the energy dissipation rate density is the main step for the extremum treatment of the problem. It has been proved[17] that the real macroscopic velocities $\vec{u}$ in the volume Θ of the body render stationary the functional

$$W = \int_\Theta (\Phi - \vec{F}\cdot\vec{u})d\Theta - \int_\Sigma (\vec{T}\cdot\bar{u})d\Sigma \tag{18}$$

where $\vec{F}, \vec{T}$ are the body force and traction at the surface Σ of the specimen. Dissipation potential Φ is calculated through the energy dissipation rate density I in the form[17]

$$\Phi = \int_0^1 I(\lambda e_{ij})\frac{d\lambda}{\lambda} \tag{19}$$

The specific problem in the modelling of material behaviour with broken necks is that the functional (16) depends on the macroscopic strain rates of the powder in two ways: on the one hand the dissipation rate density I is a function of dissipation rates at the junctures and on the other hand the number of junctures also depend on strain rates through fracture criterion (9). Indeed, if the strain rate at the juncture exceeds its critical value the juncture is considered as broken one and its area is taken out of S_i.

In general, minimization of the energy functional gives a correct solution to the problem of velocity determination only if the geometry of deformation is fixed and variation of S_i is not allowed.[18] The result of the variation of energy functional (19) with respect to S_i is equal to zero if the terms in the square brackets of (16) are equal to zero at the boundary line between $S_i$and the other part of particle surface. In that case the statement of the problem becomes similar to the classical one.[18] It is clear from (14) that terms in (16) vanish at the boundary line if $\dot{w} = 0$ at that line. According to the definition of S_i the strain rates of the junctures located at the boundary line of S_i are equal to $\dot{\varepsilon}_c$. Therefore, if $\dot{\varepsilon}_c = 0$ the functional gives correct description of the problem. The more general form of I for arbitrary $\dot{\varepsilon}_c$ can be readily obtained with the use of a similar idea. The general form of I is given in the Appendix A.

The important feature of the function Φ defined in (19) lies in the fact that in the case of correct statement of the extremum problem the stresses in powder compact can be evaluated as derivatives of Φ with respect to corresponding strain rate components

$$\sigma_{ij} = \frac{\partial\Phi}{\partial e_{ij}} \tag{20}$$

In our case the equality (20) can be checked by direct calculations of average stresses in material and subsequent comparison with the derivative of (19) with respect to strain rate component.

Indeed, the stresses in powder compact can be defined as[19]

$$\sigma_{ij} = \bar{N}\frac{1}{4\pi}\int_{S_i} w(F_in_j + F_jn_i)dn \tag{21}$$

where $\bar{N}$ is the average number of junctures per unit volume

$$\bar{N} = \frac{\rho Z}{2V} \tag{22}$$

$\overrightarrow{F}$ is the interparticle contact force and Z is the coordination number. Substitution of $F = \sigma n_i$ and relationship (1) for σ into (21) readily confirms (20).

The stress–strain rate relationship (20) is, in general, the non-linear one with respect to strain rate components despite the linear behaviour of every neck under loading. The nonlinearity is the result of the correlation between the number of broken necks and the stresses in the powder body.

4. Numerical treatment of the problem

Evolution of parameters of the powder compact during sintering was treated incrementally with the time step Δt. The numerical approach for the determination of macroscopic velocities of the powder at any moment of time was based on finite element minimization of (18). The non-linear problem was solved by iterative method. In every step of iterations the part of the particle surface with broken necks was fixed. For the fixed S_i the non-linearity in the model disappeared and velocities were found from the solution of the linear set of equations obtaining by minimization of (18). After velocity determination new S_i was calculated according to fracture criterion. The process was repeated until convergence condition was met.

The macroscopic velocities and strain rates allow calculations of $\dot{w}$ and, consequently, w for any orientation of neighbour particles. Parameter w was considered as a characteristic of the accumulated strain at the neck and it was evaluated from the equation

$$\frac{w}{R} = 1 + E_{ij} n_i n_j \tag{23}$$

where components E_{ij} of the strain tensor obeyed evolution equations

$$\frac{dE_{ij}}{dt} = e_{ij} \tag{24}$$

For simplicity the current neck radiuses were calculated through Coble's equation[12]

$$\frac{x}{R} = 2\sqrt{\frac{R - w}{R}} \tag{25}$$

The evolution of relative density of powder compact was calculated by the step-by-step procedure from the equation of mass conservation

$$\Delta\rho = -\rho e \Delta t \tag{26}$$

where e was the relative rate of volume change, $\Delta\rho$ was the increment of the relative density. The initial value of the neck radius was taken in the form[20]

$$\frac{x_0}{R} = \left(\frac{3}{2}\pi\gamma(1 - \nu^2)/E_E R\right)^{\frac{1}{3}} \tag{27}$$

where E_E was the Young modulus of material, ν was the Poisson ratio. Eq. (27) means that the appearance of non-zero initial neck is the result of elastic powder compression under the influence of initial adhesive force equal to $4\pi R\gamma$.[21]

For the analysis of numerical results it is convenient to introduce the parameter ϕ for the maximum accumulated strain over all possible orientations of the necks at the particle

$$\phi = \max_{n_i, n_j} E_{ij} n_i n_j \tag{28}$$

The relative values of ϕ normalized to their maximum magnitude in the volume of the powder compact are used in the subsequent development.

5. Sufficient condition of defect-free sintering

The fracture criterion (7) always overestimates damage level in the sintering body. At the same time, if modelling with the fracture criterion (7) does not predict existence of any residual damage after sintering, it can be treated as a sufficient condition of defect-free sintering.

As an example, the sintering of alumina was considered. The damage development during sintering of alumina layer on rigid substrate was observed in[1] at the temperature 1500°C. This was the reason for the choice of the isothermal sintering at that temperature for the modelling. Diffusion parameters of alumina powder were taken from.[22] Their values are given in the Appendix B. Substitution of the diffusion parameters into (5) gives $\xi \approx 2$. As it follows from the results of numerical modelling[12] the same value of the parameter ξ provides the best agreement of the theoretical predictions with the experimental data.[23] For that value of ξ Eq. (9) gives $\dot{\varepsilon}_c \approx 0$. Parameters in Eq. (2) were taken from.[12] In that case they were $\alpha = \frac{9}{2}$; $\beta = 4$. The average radius of powder particles was assumed equal to 1 μm.

Sintering of powder-based composites with rigid inclusions is one of the most well-known example of constrained sintering that provokes damage development.[4,5,24] As the first example of the modelling the composite specimen with the internal structure given in Fig. 2 was considered. It was the alumina powder cylinder with the sphere-like inclusion. The inclusion in homogeneous cylindrical powder specimen was treated as a rigid and friction between powder and inclusion was neglected.

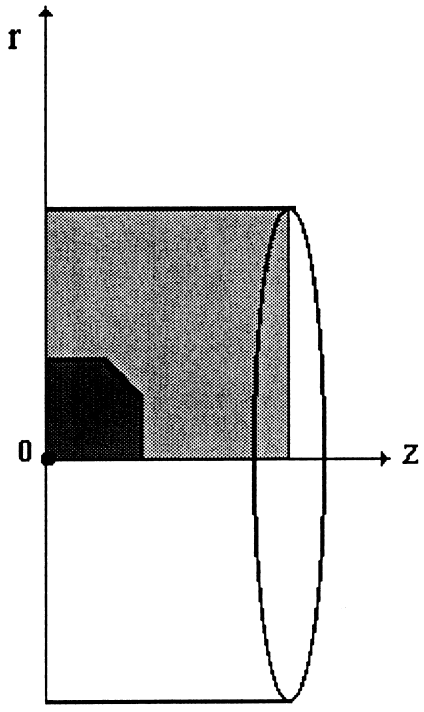

Fig. 2. Unit cell of the composite material with rigid inclusions.

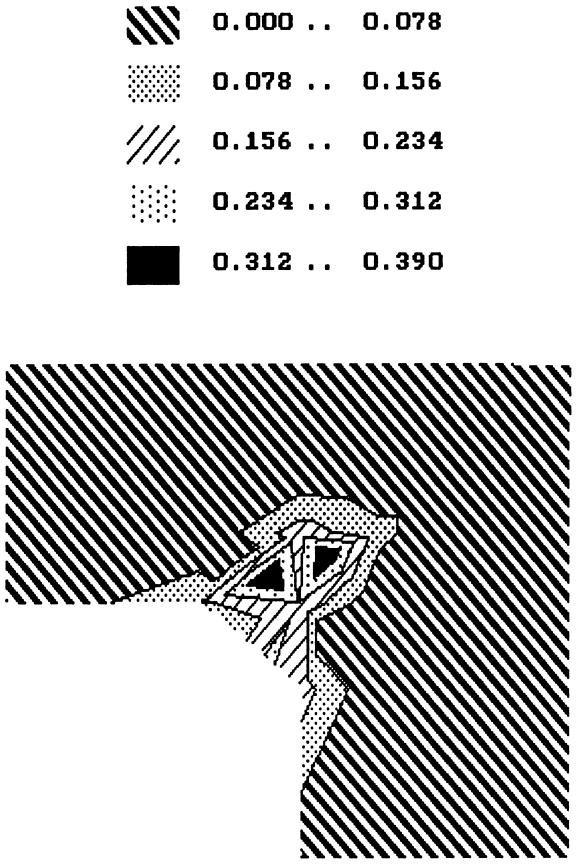

Fig. 3. Distribution of the damage parameter χ in the unit cell of the composite.

Volume distribution of the damage parameter χ for the average density of material $\rho = 0.74$ and initial density $\rho_0 = 0.64$ is given in Fig. 3. Modelling predicts that if damage zone near the inclusion is formed, this zone does not disappear with increasing density. The damage level for the given average density of the powder is a function of the volume concentration of the rigid inclusions. The damage level decreases when concentration decreases. The damage development substantially depends also on contact conditions between powder and inclusion. For example, in the case of the perfect sticking the damage zone does not reveal itself.

Another example of sintering with damage development is sintering of cylindrical powder ring with rigid cylindrical core. In the modelling no sliding was assumed between core and powder. The sintering leads to the development of the tensile strain zone at the free end of the cylinder. The volume distributions of the normalized maximum accumulated tensile strain ϕ for the cylinders with different aspect ratios are given in Fig. 4. According to the fracture criterion the accumulated tensile strain means the interface separation between rigid core and powder at the free end of the composite cylinder. It should be noted, that a damage zone is present in the specimen despite overall densification of the composite. The effect is more pronounced for the long cylinders and disappears for the short one. The average density of the cylinders in the picture is $\rho = 0.71$. The difference between the levels of accumulated tensile strains ϕ in Fig. 4a and b gives plausible explanation of the difference in observation of radial crack development for the long[5] and short cylinders.[24] Similarly to the results of modelling given in Fig. 3 the radial cracks observed in[5] can appear around the core near the free end of the cylinder only in the case of low friction between powder and core in that region. The lowest possible friction is attained when interface crack appears between the core and powder. Therefore, in this case the formation of radial cracks is inseparably connected with the formation of interface crack. If length of the cylinder is small and interface separation does not take place, the friction between powder and core prevents development of radial cracks as it was observed in.[24]

6. Influence of mesoscopic powder heterogeneity on damage development

The kinematic assumption (12) is strictly correct only for periodically packed particles. The packing of a typical powder has an irregular or random nature. The result of the irregularity is a mesoscopically nonuniform densification of powder and existence of local volumes with low strength, that can be destroyed before the moment of damage appearance in regular powder packing.

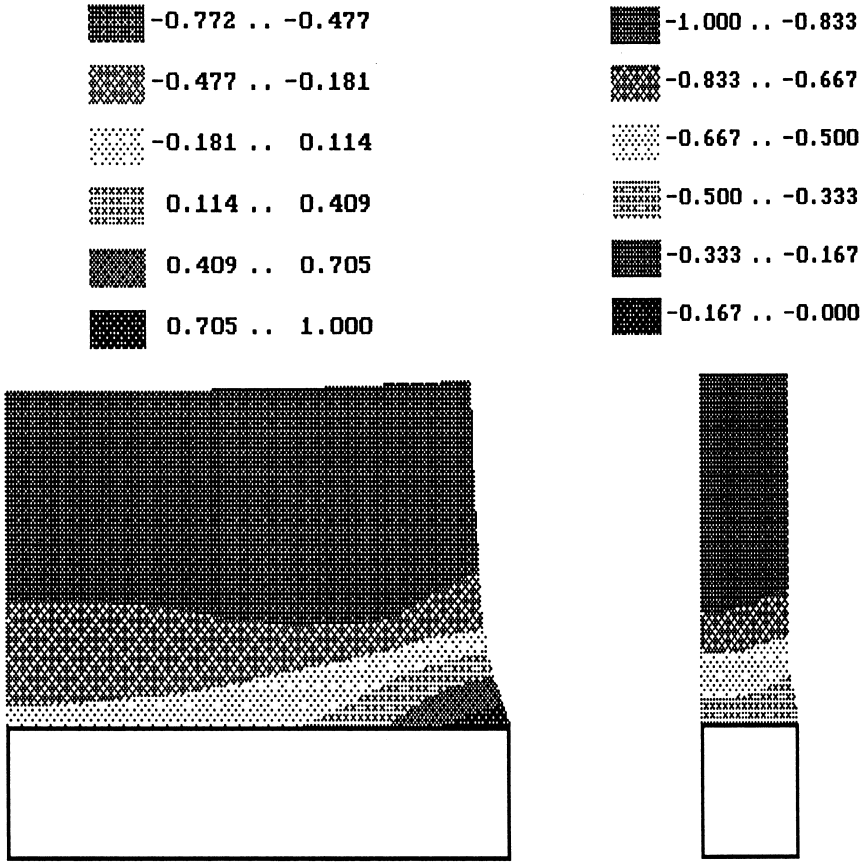

Fig. 4. Volume distribution of the relative values of the maximum accumulated strain ϕ in the powder compact: (a) long cylinder; (b) short cylinder.

According to Ref. 25 any powder body can be treated as a mixture of N types of powder packings with different bulk viscous moduli K_j, shear viscosity μ_j and free sintering rates e_{fj}. From the structural point of view the powder packings differ in co-ordination number and particle size.

The volume change rate of the jth local powder volume can be stated in the form

$$e_j = e + \Delta e_j \tag{29}$$

where e is the mean volume change rate of the powder element and Δe_j is its deviation of the volume change rate due to powder packing inhomogeneity. The relationships for Δe_j were obtained in[25] for the case of a fixed volume of the powder body. These equations can be readily extended to the more general case of consolidating powder

$$\Delta e_j = -\frac{p_j \sum_{j=1}^{N} q_j (e_{fj} - e) - q_j (e_{fi} - e) \sum_{j=1}^{N} p_j}{f_j \sum_{j=1}^{N} p_j} \tag{30}$$

where

$$q_j = \frac{3K_j f_j}{3K_j + 4\mu_m}$$
$$p_j = \frac{3f_j}{3K_j + 4\mu_m} \tag{31}$$

Here f_j stands for the volume fraction of powder packing of jth type and μ_m is the average viscous shear modulus of material. Eq. (30) provides additional information about differential densification of powder if geometrical peculiarities of the packing are known. More detail information about mesoscopic heterogeneity of the powder compact gives also chance to improve fracture criterion and conditions of defect-free sintering.

Eq. (30) predicts that during constrained sintering some local volumes of powder can dilate despite the overall densification of powder element. In experiments about densification of alumina-zirconia laminates[3] and damage development under low tensile stress[26] the damage in the form of the series of large pores was observed. The mechanism of the damage development was based on the influence of primary large pores as stress concentrators during constrained sintering. The region immediately next to the pore was a preferable place for the formation of the next pore in the series.

In order to evaluate the damage development due to mesoscopic powder inhomogeneity we shall assume that some local volumes with very low strength are always present in the powder compact. They can be, for example, large pores or powder volumes with large amount of cracks. The bulk viscous modulus can be taken equal to zero for these volumes. The initial concentration of these "weak" volumes will be treated as negligibly small.

Eq. (30) can be used for the two-phase material, where one phase consists of "weak" volumes of powder and the second phase has some mean deformational properties defined from the macroscopic model mentioned above. Substitution $f_1 = 0, f_2 = 1$ into (30) gives value of $\Delta e_1 \neq 0$.

The shear components of the strain rate tensor near the weak volumes are also different from the average ones. According to the Eshelby's equations, the change of the deviatoric components $\Delta'_1 e_{ij}$ of the strain rate tensor near the weak regions can be estimated as[27]

$$\Delta'_1 e_{ij} = \frac{\beta}{1-\beta}' e_{ij}$$
$$\beta = \frac{2}{15}\frac{4-5\nu}{1-\nu} \tag{32}$$

where ν is the viscous analogy of the elastic Poisson coefficient. At the early stages of sintering ν does not depend on the density of powder compact and is equal to 0.25.[28]

We shall assume that the damage spreads in some direction near the weak region if

$$\max_{n_i}(e_{ij} + \frac{\Delta e_1}{3}\delta_{ij} + \Delta'_1 e_{ij})n_i n_j > \dot{\varepsilon}_c \tag{33}$$

Condition (33) can be used as an improved version of fracture criterion during numerical modelling instead of (9). Physically, criteria (33) and (9) are similar, but the criterion (33) takes into account the strain-rate concentration near the weak region.

As an example of the use of the criterion (33) the sintering of alumina powder specimen with coin-shaped rigid inclusions was considered. In that case the damage zone appears near the corner of the inclusions. Volume distribution of damage parameter χ is given in Fig. 5. The average density of the compact in the picture was equal to $\rho = 0.74$. The damage appearance depends on the shape of the inclusions and their volume concentration. A larger height-to-radius ratio and higher volume concentration of the inclusions lead to higher damage level. No sliding was permitted between powder and inclusion. Note, that in this case the fracture criterion (9) does not predict any damage formation. The average bulk and shear viscosity of material was assessed through the relationships given in the Appendix C.

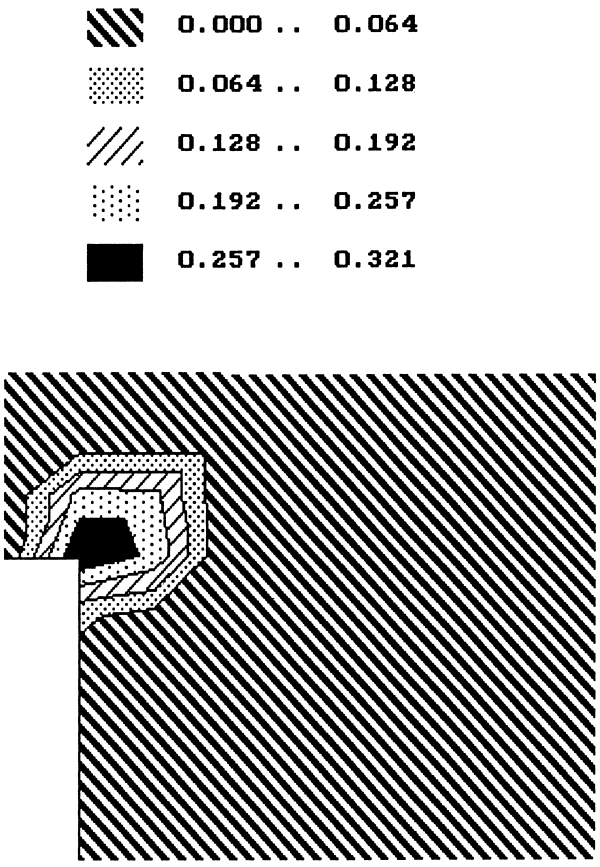

Fig. 5. Damage distribution in the unit cell of sintered composite material with the coin-shaped rigid inclusions.

The last example of the damage development during sintering has no connection with finite element calculations, nevertheless it seems important for the practical applications. The example deals with the damage appearance during sintering of a bimodal mixture of small and large alumina powder particles. Assuming that shrinkage rates at the small-to-large particle junctures are close to rates between large particles[29] the powder compact was considered as a combination of two types of volumes: the volumes of small particles that shrinks at a high rate and the rest of the powder compact that shrinks at a lower rate typical for larger particles.

Differential densification induces tensile stresses in the domains of the small particles. The level of the stresses and concomitant damage development depend on the size ratio of the powder particles. The damage appears in a powder compact when the small-to-large particle size ratio exceeds some critical value.

The critical size ratio was calculated for different compositions of the bimodal alumina mixtures. The calculations were based on the two-stage use of the relationship (30). At the first stage the average shrinkage rates in the domains of small particles without initial stress concentrators were calculated. The initial neck radiuses were assessed from (27). In the calculations the radius of

the large particles was fixed and equal to 10 μm. The ratio of the bulk viscosities in the regions of small and large particles was taken proportional to the ratio of the corresponding juncture viscosities (2) η_s, η_l and their areas A_s, A_l[30]

$$\frac{K_s}{K_l} = \frac{\eta_s A_s}{\eta_l A_l} \tag{34}$$

where K_s, K_l are the bulk viscosities of the powder compacts consisting of the small and large particles, respectively, and, in general, the indices s, l state for the parameters of the regions consisting of the small and large particles, respectively. The average shear viscosity of the material μ_m was found numerically from the equation[25]

$$\frac{f_s(\mu_s - \mu_m)}{\mu_s + \frac{\mu_m(9K_m + 8\mu_m)}{6(K_m + 2\mu_m)}} + \frac{f_l(\mu_l - \mu_m)}{\mu_l + \frac{\mu_m(9K_m + 8\mu_m)}{6(K_m + 2\mu_m)}} = 0 \tag{35}$$

where f_l, f_s are the volume concentrations of large and small particles, respectively, μ_s, μ_l are the shear viscosities of the corresponding local volumes. The ratio of the shear to bulk viscosities was treated as a constant[28]

$$\frac{\mu_l}{K_l} = \frac{\mu_s}{K_s} = \frac{3}{5} \tag{36}$$

and the average bulk modulus of the mixture was found as

$$K_m = \frac{q_l + q_s}{p_l + p_s} \tag{37}$$

where q_l, q_s, p_l, p_s where calculated from (31) for the large and small particles, respectively.

At the second stage of the calculations the initial presence of defects in the small particle domains was assumed. The application of (30) to the mixture of small particles and initial defects evaluates the increment of the dilation rate near the defects. For some critical particle size ratio the criterion (33) becomes valid in the vicinity of the defects. Results of the calculations of the critical size ratio of the particles are given in Fig. 6. Small-to-large particle critical size ratio decreases with the increase of volume concentration of small particles.

7. Conclusion

A new model for the prediction of damage accumulation during sintering is put forward. The model allows optimization of the technological process. It can predict,

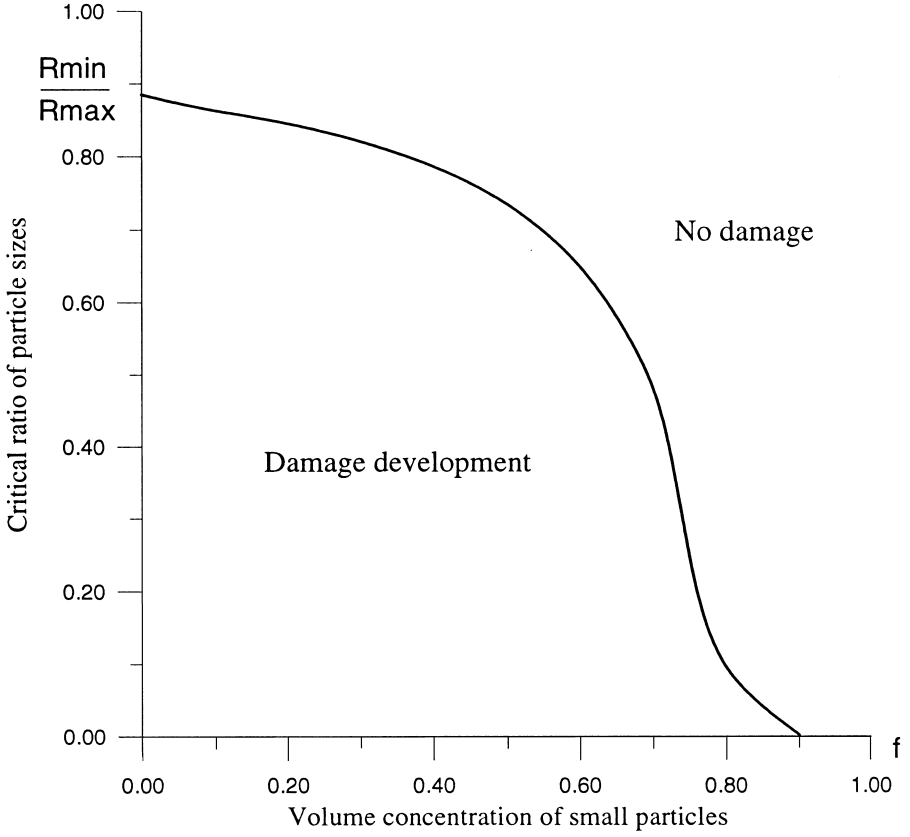

Fig. 6. Critical particle size ratio as a function of the volume concentration of small particles.

for example, the necessary level of external pressure or variation of the geometrical structure of composite to avoid damage formation. The macroscopic model of powder material with broken necks effectively predicts situations when inhomogeneous shrinkage of the powder during free sintering of particulate composites can lead to existence of the stable damaged volumes that do not disappear within the range of model validity. The theoretical approach can be extended to the case of more thorough consideration of inhomogeneity of powder packing if more detailed information about packing is available. However, the model predicts only macroscopic behaviour of the powder and can not follow in detail mesoscopic structural changes in damaged material.

Appendix A

Eq. (16) can be rewritten as

$$I = \frac{\rho\gamma}{VR}\int_S \phi_c\left[\bar{\eta}(\dot{w}-\dot{w}_c)^2 + 2\bar{\eta}\dot{w}_c(\dot{w}-\dot{w}_c) + \bar{\sigma}_0(\dot{w}-\dot{w}_c) + \bar{\sigma}_0\dot{w}_c; +\bar{\eta}(\dot{w}_c)^2\right]dS$$

where

$$\dot{w}_c = \dot{\varepsilon}_c R$$

The last two terms in the square brackets do not influence minimization if S_i is fixed and they should be dropped in our case too. All other terms vanish at the boundary line of S_i. After substitution (13) the function can be reduced to the form

$$I = \frac{\rho\gamma}{RV}\int_{S_i} \frac{\bar{\eta}w^2}{R}(e_{ij}-e^c_{ij})(e_{kl}-e^c_{kl})n_i n_j n_k n_l dS + w(e_{kl}-e^c_{kl})(\bar{\sigma}_0 + 2\bar{\eta}\dot{w}_c)n_k n_l dS \quad (37)$$

where

$$e^c_{ij} = \dot{\varepsilon}_c\delta_{ij}$$

Correctness of all transformations can be confirmed by comparison of stress components obtained from (21) with the derivatives of the potential function Φ corresponded to I.

Appendix B

Diffusion coefficients that were used in calculations.[22]

Surface diffusion coefficient at the temperature 1500°C:

$$D_s\delta_s = 1.74\times10^{-17}m^3s^{-1}$$

Grain-boundary diffusion coefficient:

$$D_b\delta_b = 2\times10^{-11}\exp(-\frac{460.5\frac{kJ}{mol}}{RT})m^3s^{-1}$$

Lattice diffusion coefficient:

$$D_v = 0.19\exp(-\frac{636.4\frac{kJ}{mol}}{RT})m^2s^{-1}$$

Appendix C

The average bulk viscosity K_m and shear viscosity μ_m were found in a way similar to proposed in.[28] K_m was calculated as

$$K_m = \frac{1}{3}(C_{1111}+C_{1122}+C_{1133})$$

where C_{ijkl} were the coefficients in the stress-strain rate relationships

$$\sigma_{ij} = C_{ijkl}e_{kl}$$

Parameters C_{ijkl} were calculated in the finite-element numerical procedure as a result of approximation (16) as a quadratic function of components of strain rate tensor. The average shear to bulk viscosity ratio was considered as a constant[28]

$$\frac{\mu_m}{K_m} = \frac{3}{5}.$$

References

1. Garino, T. J. and Bowen, H. K., Deposition and sintering of particulate films on a rigid substrate. *J. Am. Ceram. Soc.*, 1987, **70**, C315–C317.
2. Chang, T. and Raj, R., Flow generation during constrained sintering of metal-ceramic and metal-glass multilayer films. *J. Am. Ceram. Soc.*, 1989, **72**, 1649–1655.
3. Cai, P. Z., Green, D. J. and Messing, G. L., Constrained densification of alumina/zirconia hybrid laminates. I. Experimental observations of processing defects. *J. Am. Ceram. Soc.*, 1997, **80**, 1929–1939.
4. Lange, F. F. and Metcalf, M. J., Processing related fracture origins. II. Agglomerate motion and cracklike internal surfaces caused by differential sintering. *J. Am. Ceram. Soc.*, 1983, **65**, 398–406.
5. Ostertag, C. P., Charalambides, P. G. and Evans, A. G., Observation and analysis of sintering damage. *Acta Metall.*, 1989, **37**, 2077–2084.
6. Sudre, O. and Lange, F. F., Effect of inclusions on densification III. The desintering phenomenon. *J. Am. Ceram. Soc.*, 1992, **75**, 3241–3251.
7. Liniger, E. G. and Raj, R., Spatial variations in the sintering rate

of ordered and disordered particle structures. *J. Am. Ceram. Soc.*, 1988, **71**, C408–C410.
8. Weiser, M. W. and De Jonghe, L. C., Rearrangement during sintering in two-dimensional arrays. *J. Am. Ceram. Soc.*, 1986, **69**, 822–826.
9. Bordia, R. K. and Jagota, A., Crack growth and damage in constrained sintering films. *J. Am. Ceram. Soc.*, 1993, **76**, 2475–2485.
10. Hsueh, C. H., Evans, A. G., Cannon, R. M. and Brook, R. J., Visco-elastic stresses and sintering damage in heterogeneous powder compacts. *Acta Metall.*, 1986, **34**, 927–936.
11. Kuhn, L., Xu, J. and McMeeking, R., Constitutive Models for the Deformation of Powder Compacts. Computational and Numerical Technique in Powder Metallurgy, ed. D. Madan, I. Anderson, W. Freizer, P. Kumer and M. McKimpson. The Minerals, Metals and Materials Society, 1993, 123-138.
12. Bouvard, D. and McMeeking, R. M., The deformation of inter-particle neck by diffusion controlled creep. *J. Am. Ceram. Soc.*, 1996, **79**, 666–672.
13. Thoules, M. D., Effect of surface diffusion on the creep of thin films and sintered arrays of particles. *Acta Metall Mater*, 1993, **41**, 1057–1064.
14. Maximenko, A. L. and Van Der Biest, O., to be published.
15. Chu, M.-Y., De Jonghe, L. C., Lin, M. F.-K. and Lin, F. J. T., Precoarsening to improve microstructure and sintering of powder compacts. *J. Am. Ceram. Soc.*, 1991, **74**, 2902–2911.
16. Kuiken, G. D. C., Thermodynamics of Irreversible Processes. John Wiley & Sons, 1994.
17. Edelen, D. G. B., Primitive thermodynamics: a new look at the Clausius-Duhem inequality. *Int. J. Eng. Sci.*, 1974, **12**, 121–141.
18. Washizu, K., Variational Methods in Elasticity and Plasticity. Pergamon press, 1968.
19. Jagota, A., Mikeska, K. and Bordia, R. K., Isotropic constitutive model for sintering particle packings. *J. Am. Ceram. Soc.*, 1990, **73**, 2266–2273.
20. Geguzin, Ya.E., *Physics of sintering*. Nauka, Moscow, 1984.
21. Kohno, A. and Hyodo, S., The effect of surface energy on the microadhesion between solids. *J. Phys. D: Appl. Phys.*, 1974, **7**, 1243–1246.
22. Sajgalik, P., Panek, Z. and Uhrik, M., The surface diffusion coefficients of MgO and Al_2O_3. *J. Mater Sci.*, 1987, **22**, 4460–4464.
23. Coblenz, W. S., Dynys, J. M., Cannon, R. M. and Coble R. M., Initial stage solid state sintering models: a critical analysis and assessment. Proc. 5 Int. Conf. Sint. Relat. Phenom., ed. G. C. Kuczynski. Plenum Press, New York, 1980, 36-43.
24. Lange, F. F., Densification of powder ring constrained by dense cylindrical cores. *Acta Metall.*, 1989, **37**, 697–704.
25. Scherer, G. W., Coarsening in a viscous matrix. *J. Am. Ceram. Soc.*, 1998, **81**, 49–55.
26. Sglavo, V. M., Cai, P. Z. and Green, D. J., Damage in Al_2O_3 sintering compacts under very low tensile stress. *J. Mater. Sci. Lett.*, 1999, **18**, 895–900.
27. Eshelby, J. D., The determination of the elastic field of an ellipsoidal inclusion and related problems. *Proc. Roy. Soc.*, 1957, **A241**, 376–396.
28. Riedel, H., Zipse, H. and Svoboda, J., Equilibrium pore surfaces, sintering stresses and constitutive equations for the intermediate and late stages of sintering. II. Diffusional densification and creep. *Acta Metall. Mater.*, 1994, **42**, 445–452.
29. Pan, J., Le, H., Kucherenko, S. and Yeomans, J. A., A model for the sintering of spherical particles of different sizes by solid state diffusion. *Acta Mater.*, 1998, **46**, 4671–4690.
30. Maximenko, A. and Van Der Biest, O., Damage accumulation under sintering. Proc. Int. Workshop Model. Metal. Powd. Form. Processes, Grenoble, 1997, 361–370.